SUPPLEMENTAL FIGURES AND TABLE TO STAUBER AND JENTSCH

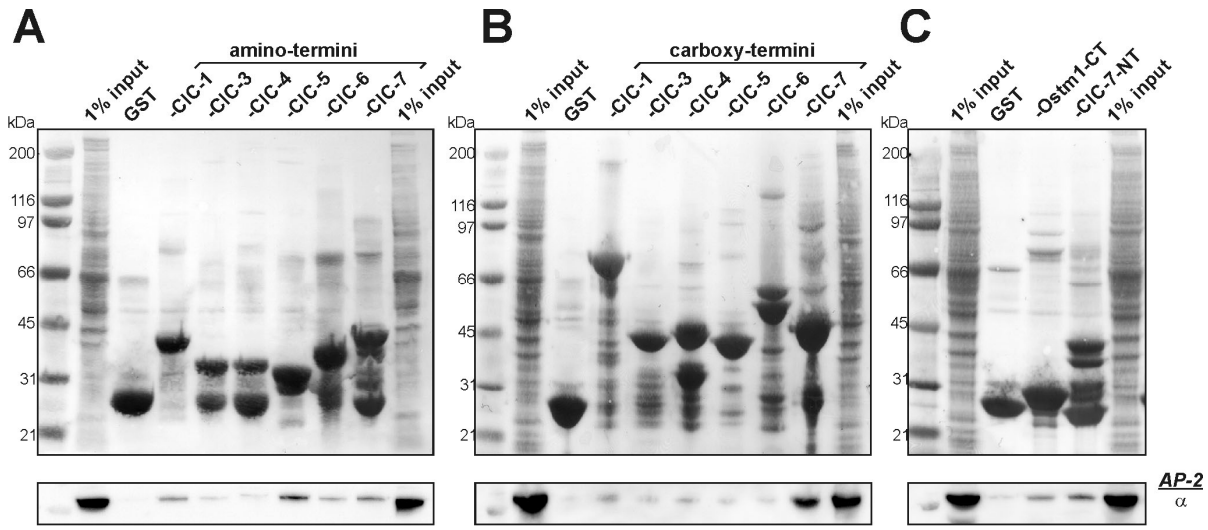

Supplemental Fig. 1. Ponceau stainings of eluates from pull-down experiments of Fig. 1 revealed that similar amounts of GST fusion proteins were used as bait. An additional immunoblot against the α-adaptin subunit of AP-2 is shown as an example of blots for further AP subunits that gave the same binding pattern as those for other subunits of the same AP complex as shown in Fig. 1A-C.

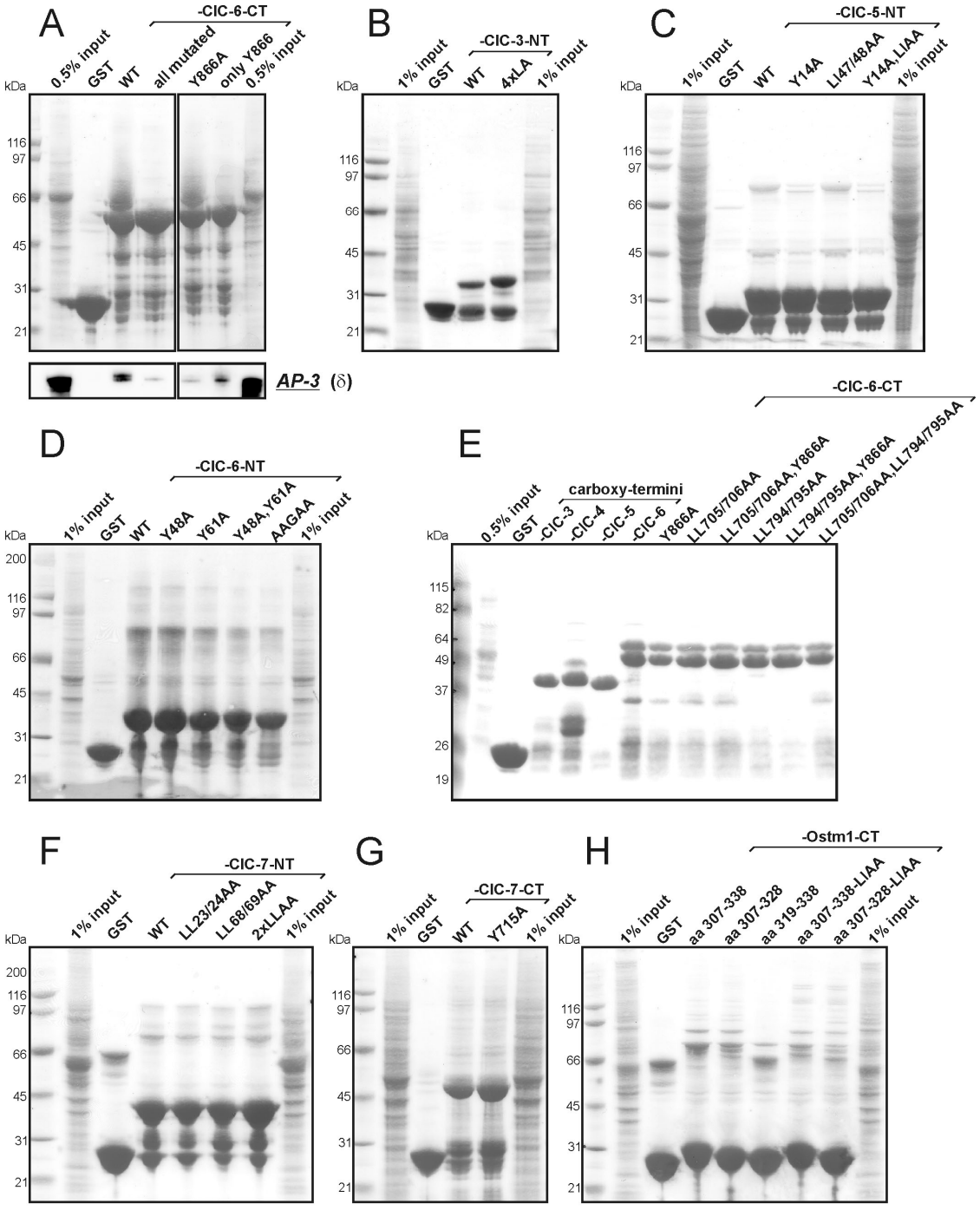

Supplemental Fig. 2. *A*, eluate of pull-down from HeLa cell extract with GST fusion proteins of the ClC-6 carboxy-terminal domain (as in Fig. 2E but with a different subset of mutants), Ponceau-stained for proteins (top) and immunoblotted for the AP-3 subunit δ-adaptin. Mutating tyrosine Y866 alone to alanine (Y866A) diminished binding of δ-adaptin as strongly as the combined mutation of the tyrosines and di-leucines, respectively, $Leu^{705}Leu^{706}$, Tyr^{717}, Tyr^{774}, Tyr^{784}, $Leu^{794}Leu^{795}$ and Tyr^{866}, to alanines (all mutated). Mutating all of these except for Tyr^{866} (only Y866) did not strongly affect binding of AP-3 compared to wildtype (WT). *B-H*, Ponceau stainings of the corresponding immunoblots shown in Fig. 2B-H revealed that similar amounts of WT constructs and point mutants of the GST fusion proteins were used as bait in the respective pull-down experiments.

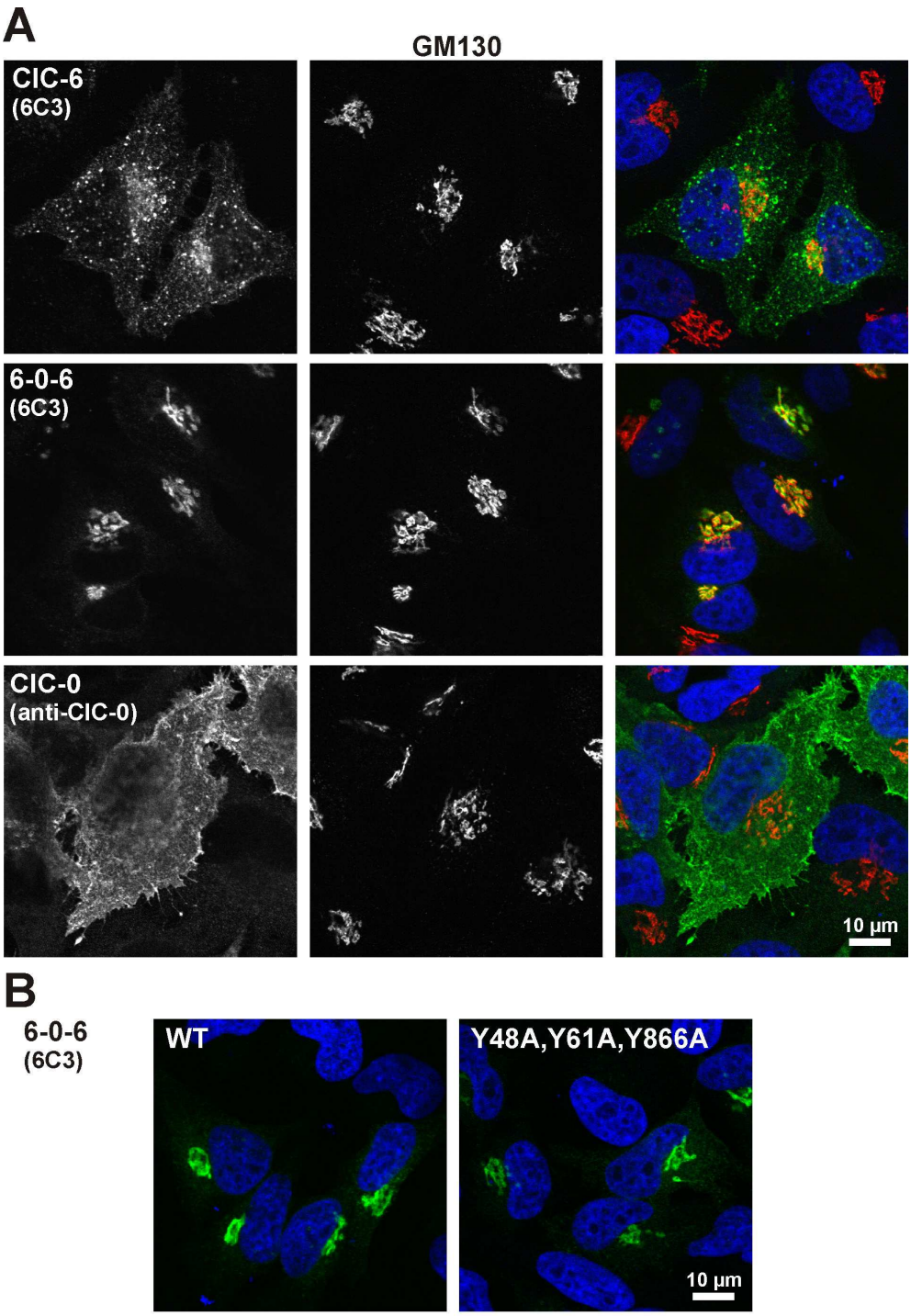

Supplemental Fig. 3. *A*, immunostaining of HeLa cells transiently expressing ClC-6, the chimera 6-0-6 (amino- and carboxy-terminal domains of ClC-6, transmembrane region of ClC-0) or ClC-0 with antibodies directed against the *cis*-Golgi marker GM130 (red in merge) and the C-terminus of either ClC-6 (ClC-6 and 6-0-6) or ClC-0 (ClC-0) (green in merge). *B*, immunostaining with an anti-ClC-6 antibody of HeLa cells expressing either the chimera 6-0-6 or the one in which tyrosines Tyr^{48}, Tyr^{61} and Tyr^{866} of the full-length ClC-6 sequence were mutated to alanines showed that the perinuclear localization of 6-0-6 is not altered by those mutations.

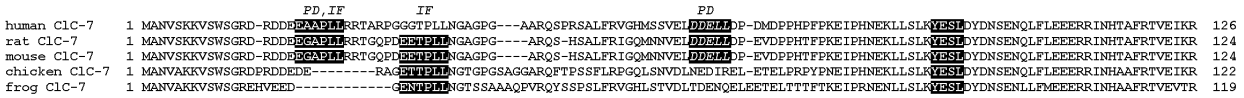

Supplemental Fig. 4. Comparison of the amino-terminal regions of ClC-7 from human, mouse, rat, chicken and frog. Potential AP-binding ([DE]XXXL[LI] and YXXΦ) and GGA-binding (DXXLL) sorting motifs are highlighted as white on black background (the latter in italics). *PD* and *IF* above a motif indicate that we showed its involvement in AP complex or GGA protein binding in our pull-down experiments with human ClC-7 and in lysosomal sorting in our subcellular localization studies with rat ClC-7, respectively.

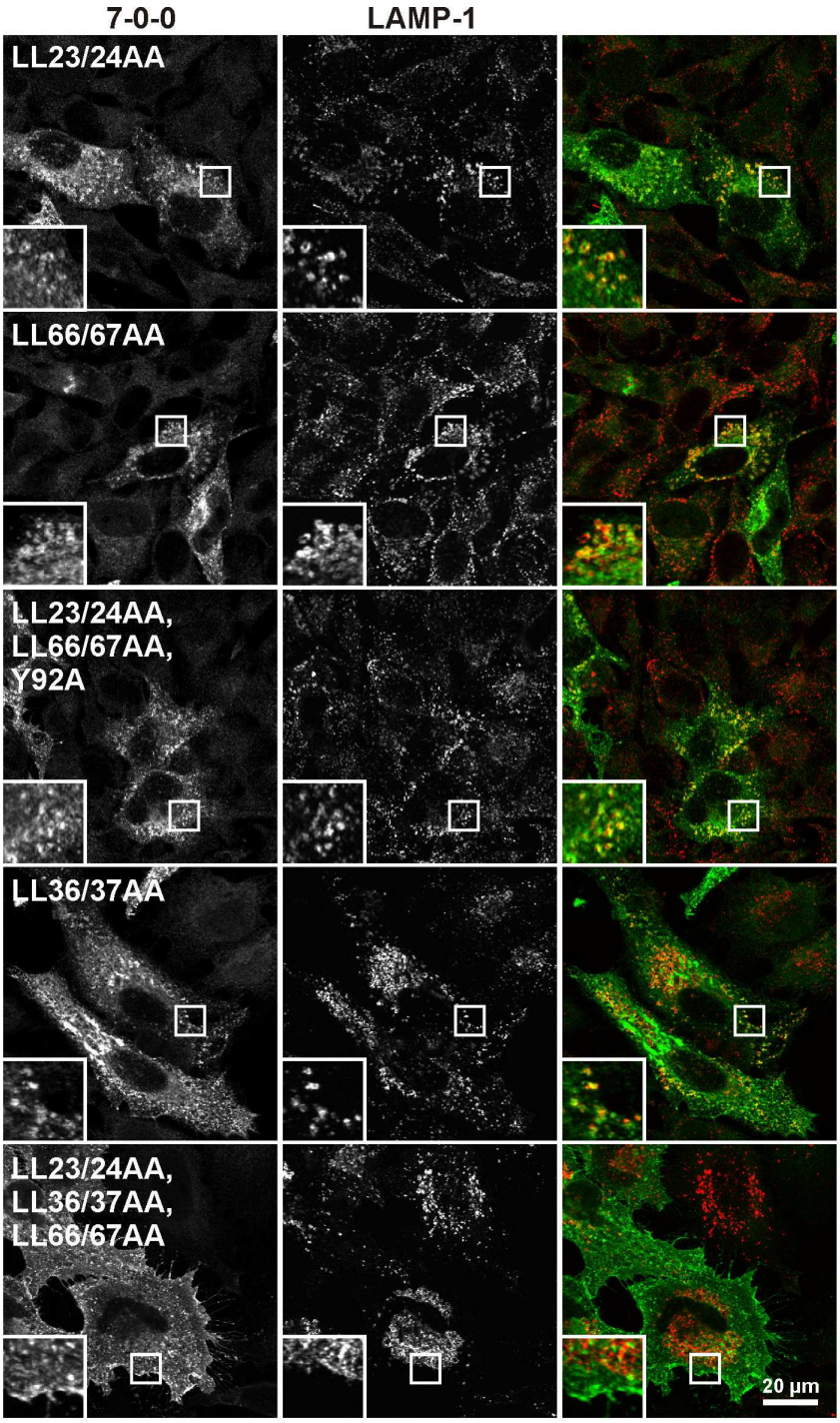

Supplemental Fig. 5. Immunocytochemistry showing subcellular localization of transfected 7-0-0 chimeras with further mutations in the ClC-7 N-terminus compared to LAMP-1 staining in HeLa cells. The amino-terminal region of ClC-0 replaced by that of rClC-7, as in Fig. 5B, but carrying different combinations of point mutations. Costaining with antibodies against the carboxy-terminal region of ClC-0 (green in merge) and the late endosomal/lysosomal marker protein LAMP-1 (red in merge) revealed that $7^{LL23/24AA}$-0-0, $7^{LL66/67AA}$-0-0, $7^{LL23/24AA,LL66/67AA,Y92A}$-0-0 and $7^{LL36/37AA}$-0-0 localized to late endosomes/lysosomes. In contrast, $7^{LL23/24AA,LL36/37AA,LL66/67AA}$-0-0 did not colocalize with LAMP-1 but reached the plasma membrane, just like the $7^{LL23/24AA,LL36/37AA,}$-0-0 chimera in Fig. 5B.

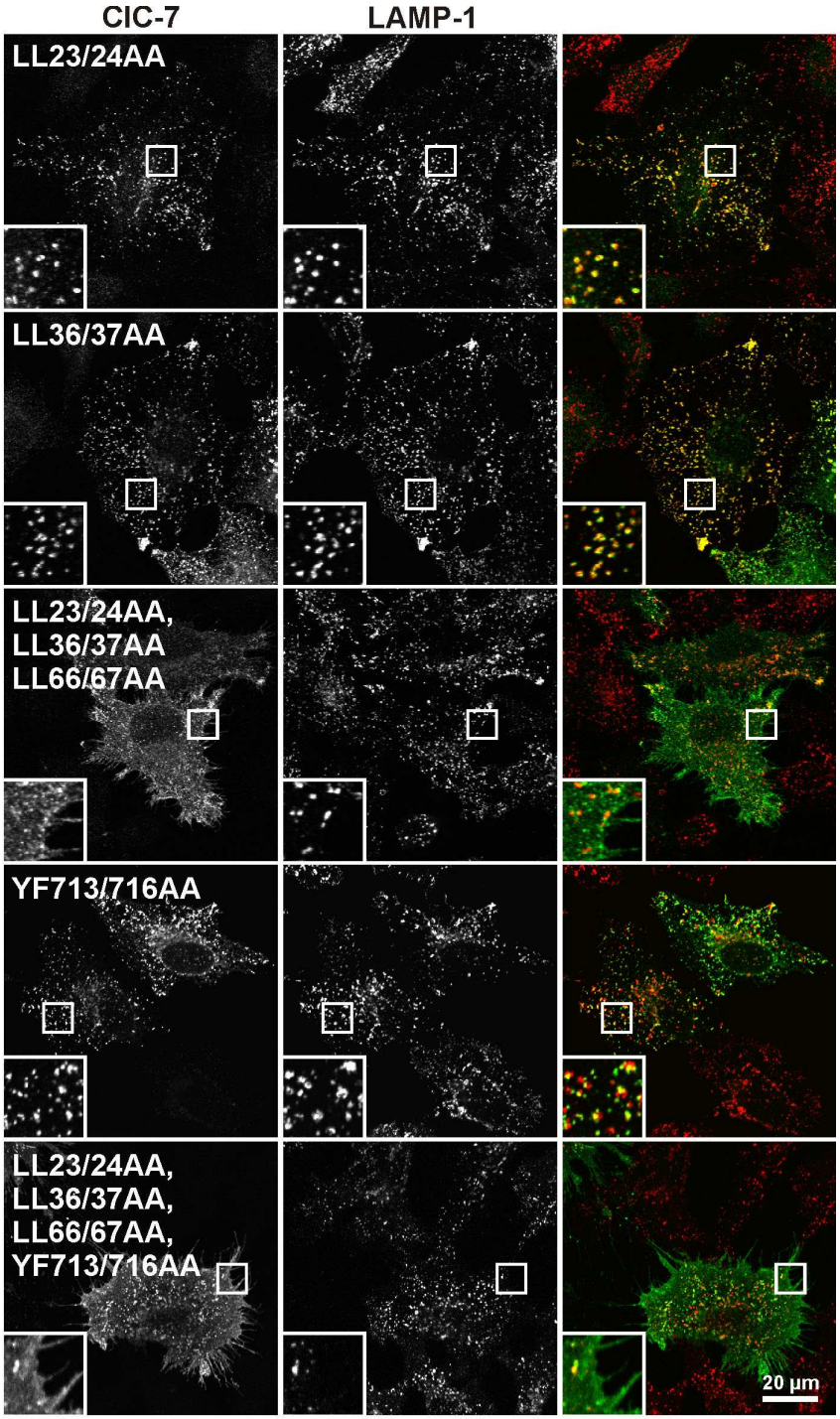

Supplemental Fig. 6. Subcellular localization of further rClC-7 mutants in transiently transfected HeLa cells, determined by immunostaining for ClC-7 (green in merge) and the late endosomal/lysosomal marker LAMP-1 (red in merge). While rClC-7$^{LL23/24AA}$, rClC-7$^{LL36/37AA}$, rClC-7$^{LL66/67AA}$ and rClC-7$^{YF713/716AA}$ almost completely colocalized with LAMP-1, rClC-7$^{LL23/24AA,LL36/37AA,LL66/67AA}$- and rClC-7$^{LL23/24AA,LL36/37AA,LL66/67AA,YF713/716AA}$-transfected cells displayed ClC-7 staining at the plasma membrane in addition to colocalization with LAMP-1.

CLC	region	motif	type	binding partner	role in sorting
ClC-3	NT	L^{13}LDLLDE	LLDL	clathrin (Fig. 2B, ref 23)	**+** (ref 23)
ClC-5	NT	Y^{14}DDF	YXXΦ	AP-2 (Fig. 2C)	**-** (Fig. 3)
ClC-5	CT	PPLPPY^{672}TPP	PY-motif	ubiquitin ligases (refs 34 and 35)	**+** (ref 34, Fig. 3)
ClC-6	NT	Y^{48}ESL	YXXΦ	AP-2, -3 (Fig. 2D)	? (Fig. 4)
ClC-6	NT	Y^{61}LEV	YXXΦ	AP-2, -3 (Fig. 2D)	? (Fig. 4)
ClC-6	CT	Y^{866}QTI	YXXΦ	AP-3 (Fig. 2E)	? (Fig. 4)
ClC-7	NT	EAAPL^{23}L^{24}	[DE]XXX[LI]	AP-1, -2, -3 (Fig. 2F)	**+** (Figs. 5 and 6)
ClC-7*****	NT	EETPL^{36}L^{37}	[DE]XXX[LI]	APs? (n.d.)	**+** (Figs. 5 and 6)
ClC-7	NT	DDEL^{68}L^{69}	DXXLL	GGAs (Fig. 2F)	**-** ? (Figs. 5 and 6)

Supplemental Table 1. Summary of the sorting motifs newly identified or confirmed in this study. For each motif, the sequence and the position within the CLC (i.e. whether located in the amino- or carboxy-terminal region of the respective CLC) and the type of sorting motif it belongs to is given. In addition it lists the binding partner(s) identified and whether a role in subcellular sorting has been shown in this and/or in previous studies (with the respective references given). ***** this motif is not present in the human sequence and therefore has not been investigated in our pull-down experiments (n.d. = not determined).